

Alternative Roles for Putative Ice-Binding Residues in Type I Antifreeze Protein[†]

Michèle C. Loewen,[‡] Heman Chao,[§] Michael E. Houston, Jr.,[§] Jason Baardsnes,[‡] Robert S. Hodges,[§] Cyril M. Kay,[§] Brian D. Sykes,[§] Frank D. Sönnichsen,^{||} and Peter L. Davies^{*,‡}

Protein Engineering Network of Centres of Excellence and Department of Biochemistry, Queen's University, Kingston, Ontario, Canada K7L 3N6, Protein Engineering Network of Centres of Excellence and Department of Biochemistry, University of Alberta, Edmonton, Alberta, Canada T6G 2S2, and Department of Physiology and Biophysics, Case Western Reserve University, Cleveland, Ohio 44106-4970

Received November 2, 1998; Revised Manuscript Received February 9, 1999

ABSTRACT: Two sets of variants of type I antifreeze protein have been synthesized to investigate the role of Leu and Asn in the activity of this 37-residue α -helix. Leu and Asn flank the central two of four regularly spaced ice-binding Thr in the $i-1$ and $i+3$ positions, respectively. All three residues project from the same side of the helix to form the protein's putative ice-adsorption site and are considered in some models to act together as an "ice-binding motif". Replacement of Asn by residues with shorter side chains resulted in either a small loss (Ala) or gain (Thr) of antifreeze activity. However, substitution of Asn by its slightly larger homologue (Gln) abolished thermal hysteresis activity. The Gln-containing peptide was very soluble, largely monomeric, and fully helical. Of the three variants in which Leu was replaced by Ala, two of the three were more active than their Leu-containing counterparts, but all three variants began to precipitate as the peptide concentration increased. None of the seven variants tested showed dramatic differences in ice crystal morphology from that established by the wild type. These results are consistent with a primary role for Leu in preventing peptide aggregation at the antifreeze protein concentrations (10 mg/mL) normally present in fish serum. Similarly the role for Asn may have more to do with enhancing the solubility of these rather hydrophobic peptides than of making a stereospecific hydrogen-bonding match to the ice lattice as traditionally thought. Nevertheless, the dramatic loss of activity in the Asn-to-Gln replacement demonstrates the steric restriction on residues in or near the ice-binding site of the peptide.

Type I antifreeze proteins (AFPs¹) are long, alanine-rich (>60 mol %), α -helical peptides found in righteye flounders (e.g. *Pleuronectes*) and some sculpins (e.g. *Myoxocephalus*) (1, 2). Different isoforms, varying in sequence, length, and activity, have been described (M_r 3300–5000). Shorthorn sculpin serum AFPs (3, 4) and the winter flounder skin isoforms (5) both have 0–3 regularly spaced Thr, contain several Lys and/or Arg residues, and are only moderately active as antifreezes. In contrast, flounder serum AFPs are more active and are made up of tandem 11-amino acid repeats with 4 or 5 regularly spaced Thr. The most abundant isoform from winter flounder serum (HPLC-6) is 37 amino acids long and contains 3 Thr-X₂-Asx-X₇ repeats, where X is generally Ala (6–8). This peptide is the most extensively studied of the type I AFPs and is typically used as a model

for investigating the structure–function relationships of AFP binding to ice.

X-ray crystallography of HPLC-6 confirmed its predicted helical nature (9) and demonstrated regular spacing of Thr, Leu, and Asx side chains in the 3-D model (10). Sicheri and Yang (10) have designated the arrangement of Leu, Thr, and Asx within the sequences LTAAN (repeated twice along the peptide) and the variant DTASD (at the N-terminus) as ice-binding motifs (IBM). The $i, i+11$ spacing of the repeating residues places them 16.5 Å apart on the same surface of the helix. This distance matches the 16.7-Å spacing between equivalent ice lattice oxygen atoms on the {20–21} plane of ice in the <01–12> direction, which are the ice-binding plane and ice-binding direction determined for winter flounder serum AFPs by ice-etching studies (11). This potential match between AFP structure and the ice surface fuelled the notion that hydrogen bonds from Thr (and to some extent Asn) are the primary interactive force for ice binding (6, 10–13). AFP adsorption to the ice surface leads directly to inhibition of ice crystal growth by the Kelvin effect (14) and results in a lowering of the nonequilibrium freezing point below the melting point (15). The difference in these two temperatures is termed thermal hysteresis and is a function of AFP concentration.

A recent structure–function study explored the role of Thr residues in type I AFP binding to ice (16). Using solid-phase synthesis to produce variants of HPLC-6, Thr in the two

[†] This work was funded jointly by A/F Protein, Inc. and the Government of Canada's Network of Centres of Excellence program supported by the Medical Research Council of Canada and the Natural Sciences and Engineering Research Council through PENCE Inc. (Protein Engineering Network of Centres of Excellence), with additional support to F.D.S. from NIH Grant GM55362. M.C.L. was the recipient of a Medical Research Council Studentship.

* To whom correspondence should be addressed: Peter L. Davies. Tel: (613) 533-2983. Fax: (613) 533-2497. E-mail: daviesp@post.queensu.ca.

[‡] Queen's University.

[§] University of Alberta.

^{||} Case Western Reserve University.

¹ Abbreviations: AFP, antifreeze protein; IBM, ice-binding motif.

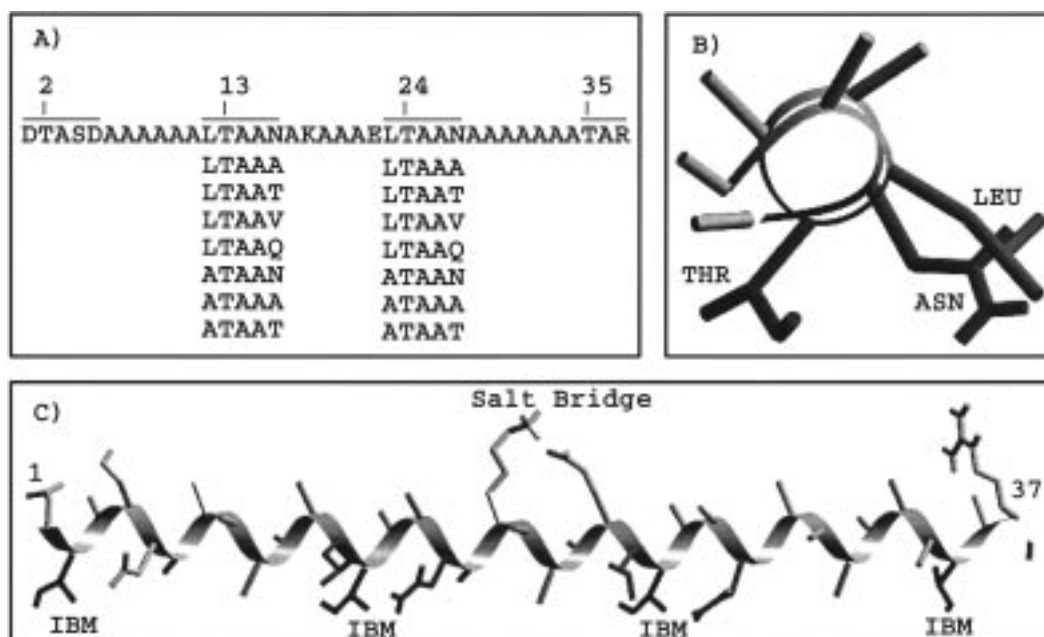


FIGURE 1: Type I AFP variant sequences and 3-D structure. (A) The wild-type sequence is shown with putative IBMs overlined and Thr identified by residue number. In all the seven variants the two central IBMs received the same alteration, which is used as a five-amino acid designation for the variant. (B) X-ray crystal structure of HPLC-6: view down a short segment of the helix from the C-terminal end showing the relative positions of the Thr, Asn, and Leu side chains in a stick and ribbon presentation (10). (C) Side view of the helix with the salt bridge and four IBM regions identified. Brookhaven Protein Data Bank identifier 1wfa.

central, identical IBMs were replaced with either Ser or Val. This double replacement magnified the effect of the change while avoiding disruption of the N- and C-terminal cap structures. A remarkable loss of activity was observed in the Ser replacement. Activity was only minimally reduced by substitution with Val, suggesting that hydrogen bonds do not dominate the ice–AFP interaction, contrary to traditional ideas. This observation was extended by Haymet et al. (17) who replaced all four Thr with either Val or Ser in a slightly modified HPLC-6 that contained two additional salt bridges for enhanced solubility (18). At 10 mg/mL the valine-substituted AFP had approximately one-half the thermal hysteresis activity of the wild type and produced the same etching patterns on ice; the serine-substituted variant was inactive.

An early structure–function study (19) probed the role of the neutral and polar residues of the IBMs. Unfortunately, due to the somewhat complex nature of the amino acid rearrangements, little could be said about Thr and Asx except that they were needed for maximum activity. The role suggested for Asx in the Wen and Laursen model was the formation of two hydrogen bonds to water molecules of a different rank than those bound by Thr (12, 19). Other models have proposed different binding arrangements for Asn, including simple penetration of the ice surface (20) and hydrogen bonding to the same rank of water molecules that Thr bind (10). In the latter model, Leu interacts with Asn to help stabilize the IBM. Another variant, where Leu from the two central IBMs was replaced with Ala, maintained only 67% of wild-type activity (19). To account for this result, Leu was suggested to stabilize AFP binding to ice via van der Waals contacts. Cheng and Merz (21) also stressed the importance of hydrogen-bonding contributions from both Thr and Asx to antifreeze activity, and they speculated on a role for the hydrophobicity of leucines in partitioning AFP to the

ice surface. However, not all models comment on the significance of either Leu or Asx to ice binding (22).

The roles of Leu and Asn become more enigmatic when the putative IBMs of other flounder serum AFP isoforms are considered. An AFP from yellowtail flounder has ATAAA and DTAAA motifs that do not conserve either the Asn or Leu residues of HPLC-6 (23). Its activity was comparable to HPLC-6 on a molar basis, which calls into question the contribution Leu and Asn make to ice binding. However, the situation is complicated by the fact that this peptide is longer, with an additional repeat (and IBM) which might help compensate for the loss of Leu and Asn. As well, a minor AFP isoform from winter flounder serum, AFP-9, has the alternative IBMs ATAAT and ATAVT that again lack Leu and Asn. It has decisively higher activity than HPLC-6 (24) but is also longer and includes an additional IBM. This isoform further emphasizes the unknown nature of the contributions of Leu and Asn and prompts the idea of developing better ice-binding motifs.

Here we have expanded on the Thr replacement study of Chao et al. (16), to explore the role of Leu and Asn in ice binding, as well as to probe the potential for designing better ice-binding motifs. We have synthesized a systematic series of seven variant peptides based on the 37-amino acid long HPLC-6 and its two central LTAAN IBMs (Figure 1). In this way we have been able to compare different IBMs without complications due to variations in peptide length or numbers of IBMs that are seen in the naturally occurring variants. Our results suggest primary roles for Asn and Leu in enhancing AFP solubility and preventing peptide aggregation.

MATERIALS AND METHODS

All the materials and methods used in this study were identical to those described in Chao et al. (16).

Table 1: Helicity of Type I AFP Variants

sample	$[\Theta]_{222\text{nm}}^a$ (deg cm ² dmol ⁻¹)	helicity (%)	T_m (°C)
LTAAN	-39 370	100	21
LTAAA	-37 250	95	28
LTAAT	-37 900	96	19
LTAAV	<i>b</i>		<i>b</i>
LTAAQ	-39 000	99	26
ATAAN	-36 060	91	21
ATAAA	-38 500	98	<i>c</i>
ATAAT	-38 200	97	20

^a The observed molar ellipticity at 1 °C. $[\Theta]$ values for ATAAN, LTAAA, and ATAAA are slightly less than 100% helical due to aggregation in solution (35). ^b The denaturation curve had multiple inflection points. T_m not determined. ^c Denaturation was irreversible. T_m not determined.

Peptide synthesis and purification were carried out in accordance with Hodges et al. (25) and Gronwald et al. (26). Circular dichroism spectra were recorded on a Jasco J-500C spectropolarimeter (Jasco, Easton, MD), and sedimentation equilibrium ultracentrifugation experiments were performed on a Beckman model E analytical ultracentrifuge, as previously described (16).

Antifreeze activity was assessed by determination of thermal hysteresis and observation of ice crystal growth by time-lapse video-microscopy. The operational definition introduced by DeLuca et al. (1996), in which an ice crystal growth rate of more than 0.2 $\mu\text{m/s}$ is defined as having reached the solution freezing point, was used throughout this study (27). The *c:a* ratios were determined by statistical analysis of between 10 and 16 crystals for each variant.

Protein concentrations were determined for all peptides by standard amino acid analysis, following activity and CD measurements.

RESULTS

Replacement of Asn: LTAAA and LTAAT. Duplicate substitutions were made in the two central ice-binding motifs (Figure 1A) to replace N16 and N27 by Ala or Thr, the two amino acids that occur naturally in these positions in some type I AFP isoforms. Neither of these changes was predicted to have a serious impact on the helicity of the AFPs. Indeed, LTAAT was fully helical at 1 °C, and LTAAA was only slightly less so (Table 1). The T_m value of LTAAT (19 °C) was comparable to that of the wild type (21 °C), but that of LTAAA (28 °C) was slightly higher. These results are in agreement with model monomeric α -helix stability data where Asn and Thr substitutions have lower T_m values than the Ala analogue (28). The elevated T_m value for LTAAA could also reflect a tendency to form multimeric complexes, particularly at higher peptide concentrations. For this reason sedimentation equilibrium analysis was performed on both variants. The experimentally determined molecular weight for LTAAT (3260) was close to the theoretical value (3217), while the average molecular weight for LTAAA (Figure 2) over the concentration range 0.7–3.1 mg/mL (3890) was higher than the theoretical value (3157) (Table 2). The plot of $\ln Y$ (concentrations in fringe displacement) versus radial distance squared (r^2) for LTAAA (Figure 2B) deviates from the expected linear relationship for a monomeric model. This suggests that LTAAA has a slight tendency to associate, and

the data are consistent with the presence of some higher order species (Table 2).

When LTAAA was assayed for thermal hysteresis activity at concentrations up to 8 mg/mL, it showed no visible signs of aggregation and was consistently 60% as active as the wild type (Figure 3A). LTAAT was 5–10% more active than the wild type over the same concentration range.

LTAAV. The increased activity of LTAAT prompted the question of whether this was due to a more favorable hydrogen-bonding arrangement or improved surface complementarity. Because valine replacement at T13 and T24 had been helpful in distinguishing between these binding interactions (16, 17), valines were substituted into LTAAT at T16 and T27. LTAAV retained appreciable activity but suffered from solubility problems at high concentrations and could not be reliably compared to LTAAT. In thermal hysteresis measurements as a function of AFP concentration, LTAAV had a maximum activity of 0.4 °C at 4 mg/mL, which was 80% of the wild-type activity (Figure 3B). At 8 mg/mL, its activity dropped to only 30% of wild-type values. Although this variant was soluble under the conditions used for sedimentation equilibrium ultracentrifugation, it exhibited significant aggregation leading to observed molecular weights between 8 000 and 16 600 (Table 2). For this reason the estimates of helix content and T_m are not reliable for this peptide. The melting curve had at least two inflection points, and the profile did not go to completion (not shown).

LTAAQ. Ala, Thr, and Val all have shorter side chains than Asn. In site-directed mutagenesis studies on the ice-binding site of type III AFP, the most deleterious mutations tended to be those that introduced a larger side chain that could sterically hinder the AFP ice interaction (27, 29, 30). In contrast, large residues could be substituted into other surfaces of the AFP without any deleterious effect on ice binding (unpublished), and no activity was lost when this AFP was fused through its N-terminus to much larger proteins (31). To probe if N16 and N27 are in contact with ice, we replaced the two Asn with Gln. The extension of these side chains by one methylene unit completely abolished thermal hysteresis activity (Figure 3A). LTAAQ was soluble up to at least 8 mg/mL. CD analysis showed that it was fully helical at 0 °C and that it had a T_m of 26 °C (Table 1). This increased stability for the Gln analogue compared to the Asn analogue (wild type) is also in complete agreement with the model monomeric α -helix stability data (28). Sedimentation equilibrium ultracentrifugation experiments suggested that LTAAQ has a slight tendency to form higher oligomeric forms. The $\ln Y$ versus r^2 plot was nonlinear (Figure 2C). However, the deviation from linearity is small, and the average molecular weight of 3644 was only marginally above the calculated value of 3242 (Table 2).

Replacement of Leu: ATAAN, ATAAT, and ATAAA. Three variants were made in which L12 and L23 were replaced by Ala: ATAAN, where only the Leu were replaced, and ATAAT and ATAAA, where N16 and N27 were also replaced by Thr and Ala, respectively, to generate IBMs found in the winter flounder AFP-9 isoform (24) and the yellowtail flounder AFP (23). When these variants were assayed for thermal hysteresis, it was apparent that all three had limited solubility at high concentrations. For this reason thermal hysteresis measurements were not made above 3 mg/mL. Up to this concentration, ATAAT was more active than

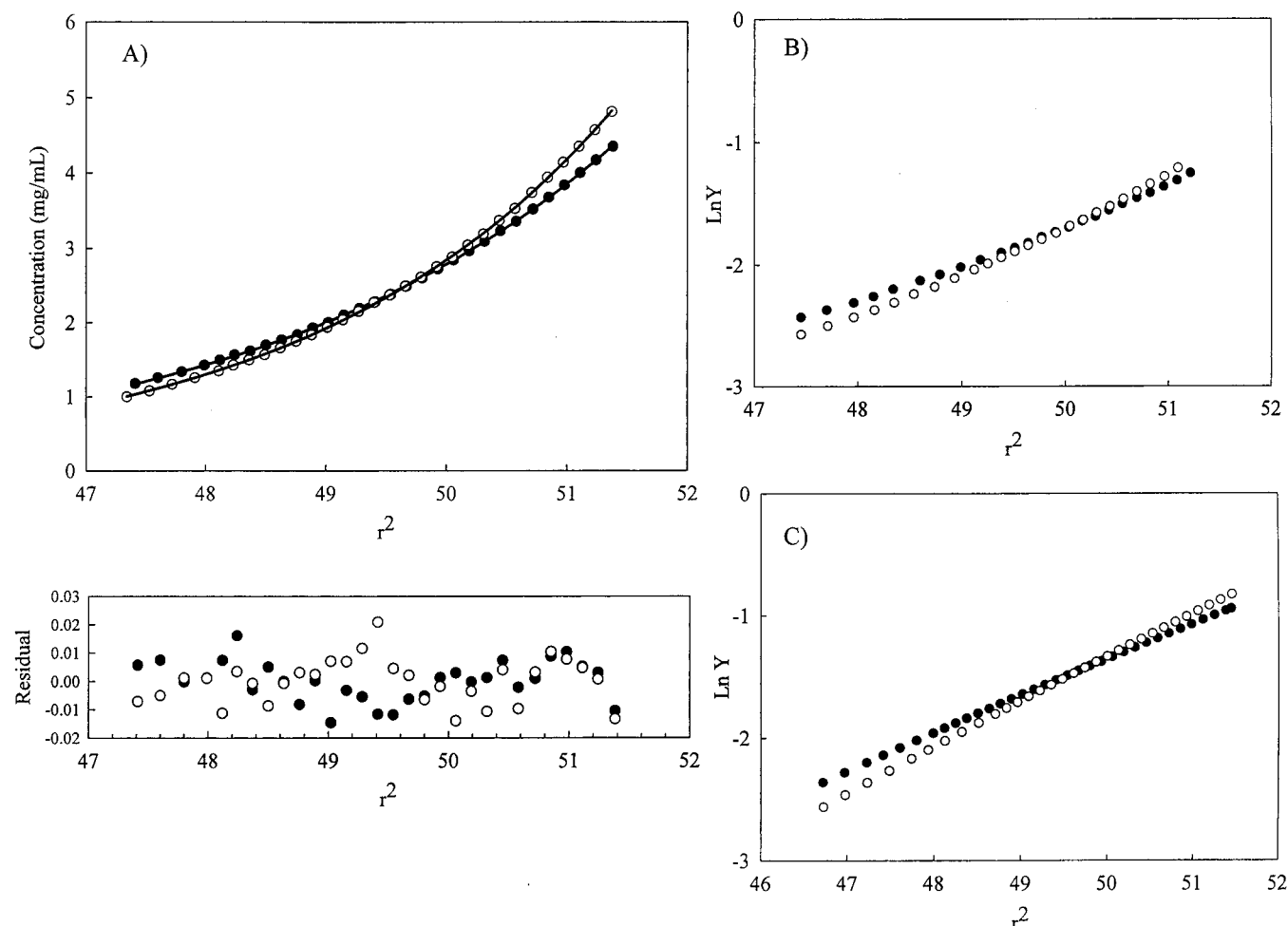


FIGURE 2: Average weight determination by sedimentation equilibrium of LTAAT (A), LTAAA (B), and LTAAQ (C). Speeds for the runs were 36 000 rpm (●) and 40 000 rpm (○). Sample loading concentration for LTAAT was 2.38 mg/mL, for LTAAA was 1.44 mg/mL, and for LTAAQ was 1.89 mg/mL. Experiments were performed at 5 °C with a phosphate buffer (50 mM KCl and 50 mM K phosphate, pH 7.0). The lower panel of A shows the result for LTAAT presented as protein concentration in mg/mL versus distance squared (r^2). The data were fitted globally to a monomer model using the program NONLIN. The fit is shown (—), and the residuals of the fit are presented in the lower panel. The results for LTAAA and LTAAQ are presented as plots of $\ln Y$ versus r^2 , where Y is concentration in fringe displacement units.

Table 2: Molecular Weight Determination by Sedimentation Equilibrium Ultracentrifugation

sample	molecular weight	
	obsd	calcd
LTAAN	3 139	3 243
LTAAA	3 890 ^a	3 157
LTAAT	3 260	3 217
LTAAY	aggregate ^b	3 213
LTAAQ	3 640	3 271
ATAAN	aggregate(nd)	3 158
ATAAA	precipitate(nd)	3 072
ATAAT	precipitate(nd)	3 132

^a Sample contained higher order species, but an average molecular weight for 0.7–3.1 mg/mL was obtained. ^b Sample aggregated (8 000–16 600).

LTAAT and ATAAA was more active than LTAAA. In contrast, ATAAN was less active than its Leu-containing counterpart (LTAAN) (Figure 3B).

Attempts to measure the molecular weight of the three variants by sedimentation equilibrium ultracentrifugation were abandoned because all three peptides precipitated slowly and irreversibly during the 3-day dialysis at 4 °C prior to the centrifugation. Molar ellipticity values for ATAAN,

ATAAT, and ATAAA were close to 100% helical, but T_m values could only be determined for ATAAN and ATAAT, because ATAAA aggregated irreversibly during thermal denaturation (Table 1).

Ice Crystal Morphology and Growth. The influence of these variant antifreeze peptides on ice crystal morphology was monitored during thermal hysteresis measurements by video-microscopy. In the presence of ATAAN, LTAAA, and ATAAA over a range of concentrations, ice crystals were hexagonal bipyramids or trapezohedrons (32) with average $c:a$ ratios close to the 3.2 (± 0.1) value observed for wild-type synthetic AFP (Figure 4). Ice crystals formed by the variant ATAAT had an average $c:a$ ratio of 2.7 (± 0.1) that was significantly shorter than the 3.2 ratio obtained with the LTAAN standard. When the Leu residue was present in LTAAT, the ratio shifted to 2.9 (± 0.5), closer to the wild-type value and not significantly different from it. The Leu residue also caused the ratio to become highly variable with a standard deviation of ± 0.5 . The ice crystals obtained with LTAAY were again not significantly different in morphology or $c:a$ ratio from those of the wild type.

One other observation about these type I AFP variants is that their ice crystals grew imperceptibly to the naked eye

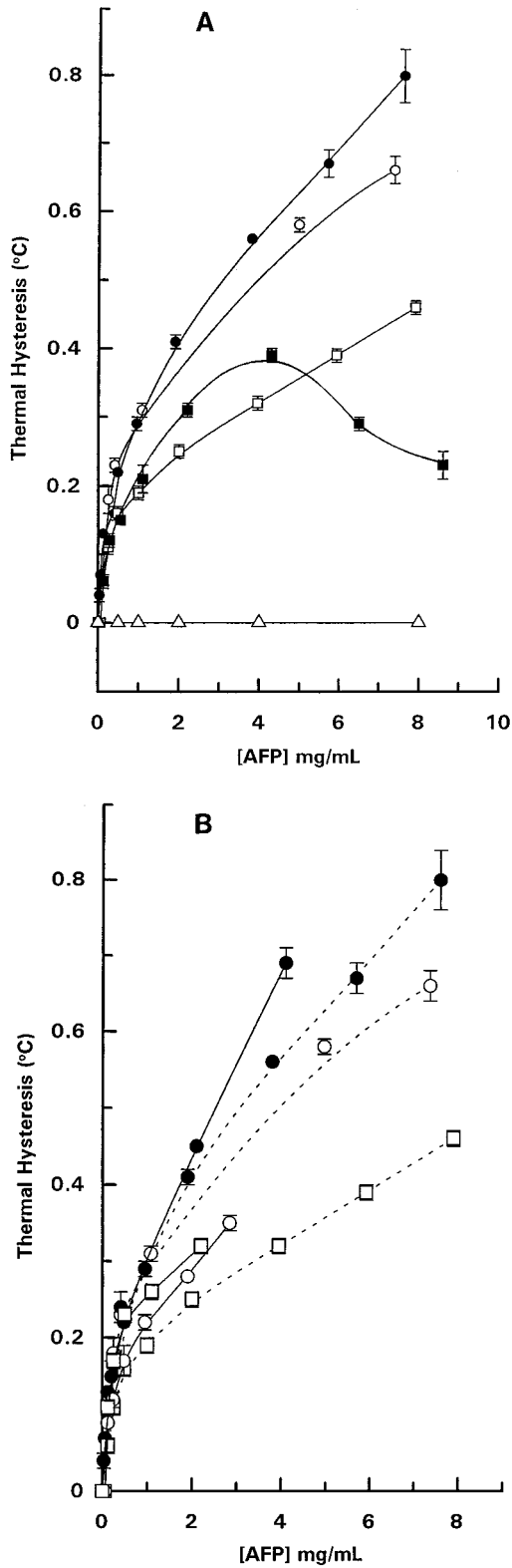


FIGURE 3: Thermal hysteresis activity of type I AFP variants. (A) Asn replacement variants: thermal hysteresis activities of wild-type HPLC-6 (LTAAN) (○), variants LTAAT (●), LTAAA (□), LTAAV (■), and LTAAQ (△) were compared over a range of concentrations. (B) Leu replacement variants: thermal hysteresis activities of ATAAT (●), ATAAN (○), and ATAAA (□) were compared over a range of concentrations. For reference, the activity profiles of their Leu-containing counterparts LTAAT (●), LTAAN (○), and LTAAA (□) are shown linked by dotted lines. Each data point represents the mean of at least three determinations. Standard deviations are shown as vertical bars.

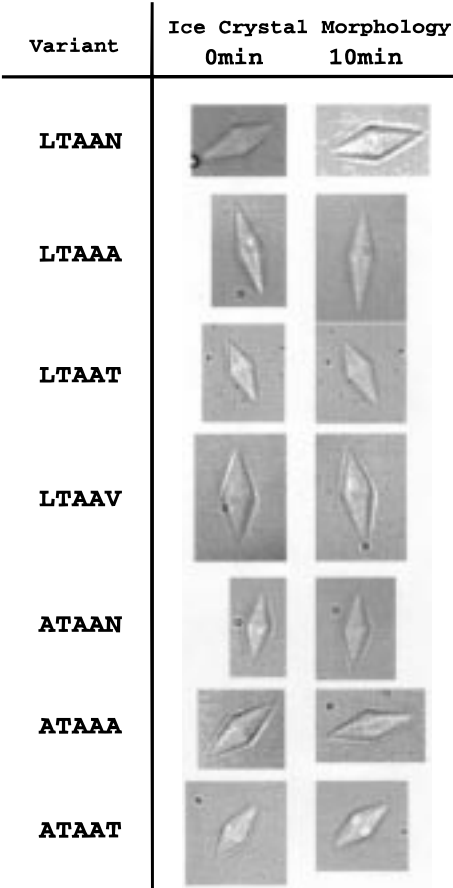


FIGURE 4: Ice crystal morphologies of type I AFP mutants. Ice crystals were formed in the presence of approximately 1 mg/mL variant AFPs at 0.1 °C cooling. Images were made at 0- and 10-min time points to evaluate the shape and growth of ice crystals over time.

during thermal hysteresis readings as the temperature was lowered. In all six cases, growth was only observed by time-lapse video-microscopy, and for all measurements made over the concentration ranges shown in Figure 3, there was a clearly defined point when crystal growth occurred suddenly and uncontrollably to mark the end of thermal hysteresis. To illustrate this point, ice crystals in the presence of 1 mg/mL peptide were held at 0.1 °C below the melting point for 10 min (Figure 4). This same phenomenon has been observed with some mutants of type III AFP (27). Mutants of both AFPs can appear to retain full activity but in some subtle way are not as good as the wild type in completely halting ice growth.

DISCUSSION

Role of Leucine. Of the six variants tested here, one (ATAAN) had previously been synthesized by Wen and Laursen (19) and found to be 67% active. This is very close to the value (70%) obtained in this study at a concentration of 1 mg/mL. The activity loss was attributed by Wen and Laursen (19) to the loss of van der Waals contacts between the Leu side chain and the ice surface in the recesses of the {20–21} plane. Another explanation, based on the crystal and solution structures, is that if Leu helps to position the Asn side chain for optimal ice binding (10) (which might also involve Asn in van der Waals contacts), then the activity loss seen with ATAAN might be partly mediated through

Asn misalignment. LTAAA, one of the variants synthesized to evaluate the contribution of Asn to type I activity, was found to have 60% of the wild-type thermal hysteresis activity at comparable concentrations. Interestingly, the double mutant (ATAAA) proved to be more active (80%) than either of the single mutants. If, as suggested by Wen and Laursen (19), Leu and Asn independently contribute to binding through van der Waals interactions and hydrogen bonding, respectively, the double mutant should have been less active than either of the single mutants. However, the 80% activity of ATAAA compared to 60% activity for LTAAA is again consistent with Leu-Asn side chain interactions. In this scenario, the absence of either side chain might release constraints on the other, freeing it to adopt a configuration less conducive to ice binding.

Visual observations indicated that all three variants with the Leu-to-Ala change had a concentration-dependent tendency to aggregate over time. Thus, the AFP activity losses for these variants could be the result of decreased solubility, and a specific ice–AFP interaction need not necessarily be proposed for Leu. Although the substitution of Leu by Ala might be expected to increase peptide solubility due to a net decrease in hydrophobicity, our results imply an overriding role for Leu in improving AFP solubility by preventing aggregation. Helices with high Ala content are prone to aggregation by coil–coil interactions. Studies have shown the existence of helical bundles, known as “Alacoils”, comprised of antiparallel coiled-coils of α -helices, with Ala in every seventh position (33). This structure allows very close spacing between helices (7.5–8.5 Å between helix axes) over four or five helical turns. It is reminiscent of leucine zippers and fibrous protein coiled-coils, except that the Alacoils are antiparallel as opposed to the parallel leucine zippers and the Alacoils are more closely packed (33). Analysis of the parameters for Alacoil formation suggests even wild-type HPLC-6 should have a propensity to form these bundles. The Leu replacement results indicate that with the removal of these side chains the propensity becomes a probability.

ATAAA, ATAAT, and ATAAN would obviously not remain in solution at the circulating AFP concentrations found in winter flounder (~10 mg/mL). And yet, ATAAA and ATAAT are IBMs that occur naturally: ATAAA in yellowtail flounder AFP and ATAAT in a winter flounder AFP isoform. Presumably there are compensating factors that keep these isoforms in solution. In the yellowtail flounder AFP, for example, there is only one ATAAA motif present out of four, and two others have Asp in place of the first Ala (DTAAA)—where Asp might serve the equivalent role to Leu. AFP-9, the isoform in flounder serum that contains the ATAAT IBM, is present there only in low concentrations despite its superior antifreeze activity.

Role of Asparagine. To test the hypothesis that Asn is involved in specific hydrogen-bonding and/or van der Waals contacts to ice, two smaller residues were introduced in its place. The loss in activity (40%) seen with LTAAA is consistent with this hypothesis, but the activity loss could also be partly due to aggregation of this peptide, possibly through the Alacoil association described above for the Leu-to-Ala replacements. Also, as mentioned above, the penalty for leaving Leu unfettered might be significant as judged by the gain in activity seen with ATAAA, despite the double

mutant's more severe aggregation tendencies. This is supported by the LTAAT and ATAAT comparison where Leu replacement was again associated with increased activity but decreased solubility.

The small but significant gain in activity seen with LTAAT is harder to reconcile with the hydrogen-bonding/van der Waals hypothesis, unless a fortuitous new hydrogen-bonding match (and/or surface complementarity) is made to the shorter side chain. This is not out of the question if water can fit onto the ice lattice at the AFP/ice interface where the Asn side chain would have been and in this position make hydrogen bond(s) to the shorter Thr side chain. (Our attempt to distinguish between a hydrogen-bonding versus space-filling role for the second Thr by swapping them for Val was inconclusive because of the solubility problems encountered with LTAAV.) However, a less complicated role for Asn could be that of a hydrophilic residue promoting the solubility of type I AFP. In this situation Thr would be a better substitution than Ala.

In the original series of type I AFP variants made by Wen and Laursen (19), Thr13 and Asn16 were swapped (variant S23) in the background of variant S11. In the present study, the superior activity of LTAAT compared to the wild type was not predictable from the Wen and Laursen mutation (where S23 had 17% activity compared to 65% for S11). This emphasizes the importance of making one type of change to the AFP at a time. On the basis of the result that Thr can substitute for Asn, the dramatic activity loss in the double mutant S23 is presumably due to the replacement of Thr13 by Asn. This is entirely consistent with the key role that Thr seems to play in type I AFP binding to ice (16, 17) and with the particular disruptiveness of larger side chains (steric effect) when introduced into the ice-binding region (27, 30).

A striking example of the steric effect was the complete elimination of activity following the Asn-to-Gln replacement (LTAAQ). This was the only variant of the Asn replacement series where a larger side chain was introduced. All the properties of LTAAQ suggest that it is a largely monomeric, fully helical, soluble peptide analogous to the wild type and that there is no trivial reason for the complete activity loss. (Indeed, the analogues with increased helix stability—LTAAQ and LTAAA—are the least active.) One interpretation of the LTAAQ result is that Asn is indeed in contact with the ice surface when type I AFP is aligned and bound to the lattice. The lengthening of the side chain by one methylene unit appears sufficient to prevent nearby, critical ice-binding residues (e.g. Thr) from contacting the ice.

A Better Ice-Binding Motif? AFP-9 contains the ATAAT IBM and is a minor isoform in winter flounder serum. This isoform has decisively higher activity on a molar basis than HPLC-6 (24), but it includes an additional 11-amino acid repeat (and IBM). Therefore, there are at least three factors that could contribute to AFP-9's superior activity: overall size, IBM type, and number of ice-binding repeats. The first of these is a valid consideration because there is clear-cut evidence that the activity of an AFP increases with its size (31). With regard to the second factor, one of the reasons for making and testing the ATAAT variant was to determine the extent to which this IBM contributes to the higher activity of AFP-9. By incorporating the ATAAT IBM into the HPLC-6 background, it was possible to eliminate the issue

of size. This variant, lacking Leu, had 20% higher activity than the wild type. The higher activity was observed immediately following resuspension and prior to any substantial aggregation. Superficially, it would seem that ATAAT is a better IBM than LTAAN, if solubility can be maintained. However, the introduction of two such IBMs in this variant inadvertently creates an additional 11-amino acid ice-binding repeat (Thr-X₁₀-Thr) partially rotated away from the main line of three repeats. We have recently shown from a minimization study that a single 11-amino acid ice-binding repeat is sufficient to bind and shape ice in a fashion similar to the full length AFP and have suggested that a single repeat may initiate the binding process (34). Thus the four ice-binding repeats of ATAAT, compared to the three in the wild type, may lead to enhanced adsorption kinetics and the observed higher activity. By the same token, AFP-9 has six repeats (4 + 2) and a slight size advantage.

This study has proposed alternative roles for Asn and Leu, two of the putative ice-binding residues in type I AFP. Leu clearly plays a critical role in preventing aggregation of these alanine-rich helices at concentrations attained in vivo. Although Asn appears to be located near the ice/protein interface, it may be more important for increasing peptide solubility than for its traditional role of contributing to binding through hydrogen bonding and/or steric complementarity.

ACKNOWLEDGMENT

We thank Paul Semchuk, Iain Wilson, and Leonard Daniels for peptide synthesis and mass spectrometry, the Alberta Peptide Institute for amino acid analyses, and Les Hicks for ultracentrifugation analysis.

REFERENCES

- Davies, P. L., and Hew, C. L. (1990) *FASEB J.* 4, 2460–2468.
- Cheng, C. C., and DeVries, A. L. (1991) *Life Under Extreme Conditions*, pp 1–14, Springer-Verlag, New York.
- Hew, C. L., Fletcher, G. L., and Ananthanarayanan, V. S. (1980) *Can. J. Biochem.* 58, 377–383.
- Chakrabarty, A., Hew, C. L., Shears, M., and Fletcher, G. (1988) *Can. J. Zool.* 66, 403–408.
- Gong, Z., Ewart, K. V., Hu, Z., Fletcher, G. L., and Hew, C. L. (1996) *J. Biol. Chem.* 271, 4106–4112.
- DeVries, A. L., and Lin, Y. (1977) *Biochim. Biophys. Acta* 495, 388–392.
- Davies, P. L., Roach, A. H., and Hew, C. L. (1982) *Proc. Natl. Acad. Sci. U.S.A.* 79, 335–339.
- Pickett, M., Scott, G. K., Davies, P. L., Wong, N., Joshi, S., and Hew, C. L. (1984) *Eur. J. Biochem.* 143, 35–38.
- Yang, D. S. C., Sax, M., Chakrabarty, A., and Hew, C. L. (1988) *Nature* 333, 232–237.
- Sicheri, F., and Yang, D. S. C. (1995) *Nature (London)* 375, 427–431.
- Knight, C. A., Cheng, C. C., and DeVries, A. L. (1991) *Biophys. J.* 59, 409–418.
- Wen, D., and Laursen, R. A. (1992) *Biophys. J.* 63, 1659–1662.
- Jorgensen, H., Mori, M., Matsui, H., Kanooka, M., Yanagi, H., Yabusaki, Y., and Kikuzono, Y. (1993) *Protein Eng.* 6, 19–27.
- Wilson, P. W. (1993) *Cryo-Lett.* 14, 31–36.
- Raymond, J. A., and DeVries, A. L. (1977) *Proc. Natl. Acad. Sci. U.S.A.* 74, 2589–2593.
- Chao, H., Houston, M. E., Hodges, R. S., Kay, C. M., Sykes, B. D., Loewen, M. C., Davies, P. L., and Sönnichsen, F. D. (1997) *Biochemistry* 36, 14652–14660.
- Haymet, A. D. J., Ward, L. G., Harding, M. M., and Knight, C. A. (1998) *FEBS Lett.* 430, 301–306.
- Chakrabarty, A., and Hew, C. L. (1991) *Eur. J. Biochem.* 202, 1057–1063.
- Wen, D., and Laursen, R. A. (1992) *J. Biol. Chem.* 267, 14102–14108.
- Madura, J. D., Wierzbicki, A., Harrington, J. P., Maughon, R. H., Raymond, J. A., and Sikes, C. S. (1994) *J. Am. Chem. Soc.* 116, 417–418.
- Cheng, A., and Merz, K. M. (1997) *Biophys. J.* 73, 2851–2873.
- Chou, K.-C. (1992) *J. Mol. Biol.* 223, 509–517.
- Scott, G. K., Davies, P. L., Shears, M. A., and Fletcher, G. L. (1987) *Eur. J. Biochem.* 168, 629–633.
- Chao, H., Hodges, R. S., Kay, C. M., Gauthier, S. Y., and Davies, P. L. (1996) *Protein Sci.* 5, 1150–1156.
- Hodges, R. S., Semchuk, P. D., Taneja, A. K., Kay, C. M., Parker, J. M. P., and Mont, C. T. (1988) *Pept. Res.* 1, 19–30.
- Gronwald, W., Chao, H., Reddy, D. V., Davies, P. L., Sykes, B. D., and Sönnichsen, F. D. (1996) *Biochemistry* 35, 16698–16704.
- DeLuca, C. I., Chao, H., Sönnichsen, F. D., Sykes, B. D., and Davies, P. L. (1996) *Biophys. J.* 71, 2346–2355.
- Monera, O. D., Sereda, T. J., Zhou, N. E., Kay, C. M., and Hodges, R. S. (1995) *J. Pept. Sci.* 1, 319–329.
- Chao, H., Sönnichsen, F. D., DeLuca, C. I., Sykes, B. D., and Davies, P. L. (1994) *Protein Sci.* 3, 1760–1769.
- DeLuca, C. I., Davies, P. L., Ye, Q., and Jia, Z. (1998) *J. Mol. Biol.* 275, 515–525.
- DeLuca, C. I., Comley, R., and Davies, P. L. (1998) *Biophys. J.* 74, 1502–1508.
- Deng, G., Andrews, D. W., and Laursen, R. A. (1997) *FEBS Lett.* 402, 17–20.
- Gernet, K. M., Surles, M. C., Labeau, T. H., Richardson, J. S., and Richardson, D. C. (1995) *Protein Sci.* 4, 2252–2260.
- Houston, M. E., Chao, H., Hodges, R. S., Sykes, B. D., Kay, C. M., Sönnichsen, F. D., Loewen, M. C., and Davies, P. L. (1998) *J. Biol. Chem.* 273, 11714–11718.
- Schultz, J. M., Qian, H., York, E. J., Stewart, J. M., and Baldwin, R. L. (1991) *Biopolymers* 31, 1463–1470.

BI982602P